

Optical Engineering

SPIDigitalLibrary.org/oe

Weighted root mean square approach to select the optimal smoothness parameter of the variational optical flow algorithms

Zhigang Tu
Wei Xie
Wolfgang Hürst
Shufen Xiong
Qianqing Qin

Weighted root mean square approach to select the optimal smoothness parameter of the variational optical flow algorithms

Zhigang Tu

Wuhan University
School of Electronic Information
Wuhan 430079, China
and
Utrecht University
School of Information and Computing Sciences
3584 CC Utrecht, Netherlands

Wei Xie

Wuhan University
Computer School
Wuhan 430079, China
E-mail: wxie.imageprocessing@gmail.com

Wolfgang Hürst

Utrecht University
School of Information and Computing Sciences
3584 CC Utrecht, Netherlands

Shufen Xiong

HuaWei Company
Shenzhen 518129, China

Qianqing Qin

Wuhan University
State Key Laboratory of Information Engineering
in Surveying
Mapping and Remote Sensing
Wuhan 430079, China

Abstract. Variational methods are the most widely used approaches for optical flow computation. Many complicated algorithms have been proposed to improve their performance, yet little work has focused on how to select the optimal smoothness parameter λ of the variational optical flow algorithm itself. We present a weighted root mean square error method to automatically select the optimal smoothness parameter λ . Furthermore, we detail a scientific method for selecting the reference λ_0 based on the quality of the frame, and propose an efficient brute-force approach to assign a group of λ , that will reduce the number of λ candidates to be tested by cutting down the search range. Experimental results validate the effectiveness of our methods. © 2012 Society of Photo-Optical Instrumentation Engineers (SPIE). [DOI: 10.1117/1.OE.51.3.037202]

Subject terms: variational optical flow; optimal smoothness parameter λ ; reference λ_0 ; weighted root mean square.

Paper 111194 received Sep. 25, 2011; revised manuscript received Jan. 9, 2012; accepted for publication Jan. 10, 2012; published online Mar. 26, 2012.

1 Introduction

Motion estimation is a fundamental problem in computer vision. Since Horn and Schunck (HS)¹ proposed the classical variational optical flow method, it has become one of the most successful approaches to obtain accurate motion information.² Motion field is the two-dimensional projection of the three-dimensional motion of surfaces in the world, whereas the optical flow is the apparent motion of the brightness patterns in the image.³ Currently, the optical flow method is widely used for motion estimation (image alignment and registration), motion analysis (object detection, object tracking, object recognition), etc.

Over the past 30 years, researchers have devised various optical flow methods. However, variational approaches have become predominant because of the following inherent advantages: 1. Integrating different concepts into one single minimization framework to combine the merits of different available approaches; 2. Using convex and robust energy functional guarantees the objective function has an unique global minimum; 3. The filling-in effect yields a dense flow field, whereas

other optical flow techniques require subsequent postprocessing steps to interpolate the sparse flow; 4. Combining with numerical approaches (multigrid method⁴) and advanced computer techniques² allows for real-time application.

Although variational methods have some superiorities, their basic structure, where a local, gradient-based matching of pixel brightness values is combined with a global smoothness assumption, has some shortcomings. Newer approaches have steadily overcome these limitations. The modified isotropic and anisotropic smoothness term,^{5,6} nonquadratic data term,⁷ and the total variation (TV) L1-norm model⁸ have been proposed to allow for piecewise smoothness, while preserving discontinuities. Outliers are penalized less severely by robust statistic functions,^{5,7} and filtering approaches have been presented to further dispose noise.⁸ Illumination change problems can be handled by integrating the assumption of constancy of the gradient or higher order derivatives,⁶ by photometric invariant constraints, by using cross-correlation techniques,⁹ or by structure-texture decomposition method² coarse-to-fine strategies,¹⁰ nonlinearized models,⁶ and descriptor matching¹¹ have been introduced to tackle large displacements. Real-time performance can be achieved by using multigrid strategy

and parallel computation in central processing units (CPU),⁴ and modern graphic processing units (GPUs).²

Most related work has focused on finding complex ways to improve the quality of the optical flow field, which in many cases only work under special conditions. In this paper, we address the problem of how to select the optimal smoothness parameter λ of the variational optical flow algorithm itself. Choosing an appropriate λ is critically important for obtaining desirable results. In Ref. 12, a smoothness weight selection problem based on the weighted distance using the blurring operator is studied, but it cannot be applied directly to variational algorithms because of its spatially varying character. A brute-force method is proposed in Ref. 13. However, it is computationally expensive, especially with respect to robust data terms. An approach jointly estimating the flow and the model parameters in a Bayesian framework is presented in Ref. 14, but this method for minimizing the objective function is too complex. Recently, Zimmer proposed an optimal prediction principle (OPP) method,⁶ but it is limited to conditions with constant speed and linear trajectories of objects.

In this paper, we introduce the Euclidean distance L2 norm-root mean square (RMS) error, which is used as a judgment to evaluate the performance of different kinds of Lucas-Kanade algorithms¹⁵ in order to determine the optimal λ . Because this approach would be challenged under some less than optimal conditions, we further modify the RMS criterion by introducing a weighting factor. Our Weighted RMS method based on the principle that the worse the flow field is, the larger the weighted RMS (WRMS) becomes, and the better the flow field is, the smaller the WRMS will be.

Section 2 describes a classical TV-L1 optical flow algorithm. Section 3 gives the detailed instruction of the WRMS approach to select the optimal smoothness parameter λ . Experimental results and corresponding analysis are provided in Sec. 4. The paper is concluded in Sec. 5.

2 TV-L1 Optical Flow Method

2.1 L2-Norm: Original Horn-Schunck Algorithm

The HS model, proposed by Horn and Schunck,¹ is based on the brightness constancy assumption which assumes the brightness of a pixel remains the same for a small motion in a short period of time:

$$I_1(x, y, t) = I_2(x + u, y + v, t + dt), \quad (1)$$

where $(u, v) = \left(\frac{dx}{dt}, \frac{dy}{dt}\right)$ are the horizontal and vertical displacement fields. Obviously, the single Eq. (1) with two unknowns (u, v) results in an under-determined equation. Besides this problem, a small perturbation in the image may create large fluctuations on its derivatives. To overcome these two problems, researchers have introduced additional constraints. Based on the type of constraints, there are two primary groups: one applies global constraints,^{1,4} another utilizes local constraints.^{10,15} The global smoothness constraint originally used in the HS model is defined as:

$$|\nabla u|^2 + |\nabla v|^2 = \left(\frac{\partial u}{\partial x}\right)^2 + \left(\frac{\partial u}{\partial y}\right)^2 + \left(\frac{\partial v}{\partial x}\right)^2 + \left(\frac{\partial v}{\partial y}\right)^2. \quad (2)$$

This smoothness constraint supposes that the neighbors of one pixel have almost the same velocity, so the flow field

varies smoothly. Then the basic L2-Norm variational algorithm is established by:

$$E(u, v) = \int_{\Omega} \underbrace{[I_2(x + u, y + v, t + dt) - I_1(x, y, t)]^2}_{\text{data term}} d\Omega + \lambda \int_{\Omega} \underbrace{(|\nabla u|^2 + |\nabla v|^2)}_{\text{smoothness term}} d\Omega. \quad (3)$$

2.2 L1-Norm: Classic+NL Algorithm

As stated in Refs. 8 and 9, in contrast to L2-norm model, the L1-norm model is better for preserving discontinuities, and also handles noise and outliers more robustly. After Rudin¹⁶ introduced the TV approach into computer vision field, the L1-norm model became the main trend in optical flow algorithms. In this work, we further improve the performance of the variational optical method by combining the representative state-of-the-art TV-L1 “Classic+NL” algorithm⁸ with our WRMS approach. The original “Classic+NL” algorithm is defined as follow:

$$E(u, v) = \sum_{i,j} \left\{ \rho_D [I_1(i, j) - I_2(i + u, j + v)] + \lambda [\rho_S(|u_x|) + \rho_S(|u_y|) + \rho_S(|v_x|) + \rho_S(|v_y|)c] \right\} + \lambda' (\|u - \hat{u}\|^2 + \|v - \hat{v}\|^2) + \sum_{i,j} \sum_{i',j' \in N_{i,j}} w_{i,j,i',j'} (|\hat{u}_{i,j} - \hat{u}_{i',j'}| + |\hat{v}_{i,j} - \hat{v}_{i',j'}|), \quad (4)$$

where λ, λ' are the weighting parameters, which control the relative importance of each term. In Sec. 3, we will propose a WRMS approach to automatically determine the optimal smoothness weighting parameter λ . $\rho(x) = (x^2 + \varepsilon^2)^\alpha$ is the slightly nonconvex penalty function, $\alpha = 0.45$, $\varepsilon = 0.001$. \hat{u} and \hat{v} are the auxiliary flow fields of u and v , and approximate to u, v . $N_{i,j}$ is the set of neighbors of pixel (i, j) in a possibly large area. $w_{i,j,i',j'}$ is the weighting parameter of the last nonlocal term, it denotes the similarity between pixel (i, j) and its neighbor pixels. In this work, $w_{i,j,i',j'}$ is modified by integrating the information about image structure and flow boundaries in order to prevent over-smoothing across boundaries. It can be calculated through their color-value distance, spatial distance, and occlusion state:

$$w_{i,j,i',j'} \propto \exp \left\{ -\frac{|i - i'|^2 + |j - j'|^2}{2\sigma_1^2} - \frac{|I(i, j) - I(i', j')|^2}{2\sigma_1^2} \right\} \times \frac{o(i', j')}{o(i, j)}, \quad (5)$$

where $I(i, j)$ is the color vector in the lab space, $\sigma_1 = \sigma_2 = 7$, $o(i, j)$ is the occlusion variable which can be calculated using Eq. (22) from Ref. 17.

2.3 Efficient Approaches to be Adopted in Solving the Algorithm

Illumination changes create common and difficult issues in motion estimation. Zimmer, Bruhn and Weickert⁶ employ the constancy of the gradient (or higher order derivatives)

method to dispose of this problem. However, the selection of the suitable weighting factor between the brightness term and the gradient term is not a trivial problem. To solve it, we apply the structure-texture decomposition method² to preprocess the input images to overcome illumination changes. A coarse-to-fine scheme¹⁰ is adopted to handle large displacement. The graduated nonconvexity (GNC) method is employed for converting the objective functional into a convex approximation. The preminent numerical method,² which is based on a dual formulation of the TV energy, is utilized to solve the optical flow algorithm. Firstly, we decompose the energy functional Eq. (4) into Eqs. (6) and (7), then update either u, v or \hat{u}, \hat{v} to get the final optical flow field (u, v) by alternatively computing the two equations:

$$E(u, v) = \sum_{i,j} \{ \rho_D [I_1(i, j) - I_2(i + u, j + v)] + \lambda \rho_S (|\nabla u| + |\nabla v|) \} + \lambda' (\|u - \hat{u}\|^2 + \|v - \hat{v}\|^2), \tag{6}$$

$$E(u, v) = \lambda' (\|u - \hat{u}\|^2 + \|v - \hat{v}\|^2) + \sum_{i,j} \sum_{i',j' \in N_{ij}} w_{i,j,i',j'} (|\hat{u}_{i,j} - \hat{u}_{i',j'}| + |\hat{v}_{i,j} - \hat{v}_{i',j'}|). \tag{7}$$

The approach described in Ref. 2 is adopted to solve Eq. (7), and the traditional SOR method combined with the nonlinear full approximation scheme (FAS)^{4,11} are used to solve Eq. (6) (SOR method is a good compromise between simplicity and efficiency). We perform three times of alternating to solve Eqs. (6) and (7) after every warping in the computing procedure.

3 WRMS Method to Select the Optimal Smoothness Parameter

Researchers introduced the smoothness assumption constraint^{1,4} to overcome the ill-posed problem in variational algorithms. The smoothness weight λ plays an important role in controlling the trade-off between the data term and the smoothness term. If λ is too small, it will result in overfitting between the two frames. If λ is too large, the flow field would be too smooth.

3.1 RMS Approach

Finding an available approach to determine the optimal smoothness parameter λ would directly improve the quality of the flow field. However, most of the present algorithms^{8,11} simply set the smoothness parameter λ to a constant. Some strategies have been adopted to handle this problem, however, each of them has some drawbacks (e.g., being computational expensive^{13,14}, being limited to special condition.⁶ By summarizing the relevant research of others, we propose a RMS approach to determine the optimal smoothness parameter λ automatically.

Simon¹⁵ employed the basic Euclidean distance error-RMS error as a measurement to judge the quality of the flow field of all kinds of Lucas-Kanade (LK) algorithms:

$$RMS = \sqrt{\frac{\sum_{x=1}^M \sum_{y=1}^N [I_1 - I_2(x + u, y + v)]^2}{MN}}, \tag{8}$$

where M, N are the number of columns and rows of the frame respectively. (u, v) are the estimated optical flow field. This measurement has been demonstrated to evaluate the performance of LK algorithms effectively by comparing the value of RMS without knowing the ground truth.

Obviously, HS variational algorithms share the same characteristic with LK algorithms—the better the smoothness parameter λ is, the more accurate the result for the optical flow field (u, v) , the better match that can be achieved between the two frames, the smaller of the RMS will be. Consequently, the optimal λ corresponds to the minimal RMS. Based on this theory, we introduce the RMS measurement to determine the optimal λ by:

$$RMS(u_{\lambda_i}, v_{\lambda_i}) = \sqrt{\frac{\sum_{x=1}^M \sum_{y=1}^N [I_1 - I_2(x + u_{\lambda_i}, y + v_{\lambda_i})]^2}{MN}}, \tag{9}$$

where $(u_{\lambda_i}, v_{\lambda_i})$ is the estimated flow field with different λ_i ($i = 1, 2, \dots$) of the variational algorithm:

$$E(u_{\lambda_i}, v_{\lambda_i}) = \sum_{i,j} \left\{ \rho_D [I_1(i, j) - I_2(i + u_{\lambda_i}, j + v_{\lambda_i})] + \lambda_i [\rho_S (|u_{\lambda_i,x}|) + \rho_S (|u_{\lambda_i,y}|) + \rho_S (|v_{\lambda_i,x}|) + \rho_S (|v_{\lambda_i,y}|)] + \lambda' (\|u_{\lambda_i} - \hat{u}_{\lambda_i}\|^2 + \|v_{\lambda_i} - \hat{v}_{\lambda_i}\|^2) + \sum_{i,j} \sum_{i',j' \in N_{ij}} w_{i,j,i',j'} (|\hat{u}_{\lambda_i,i,j} - \hat{u}_{\lambda_i,i',j'}| + |\hat{v}_{\lambda_i,i,j} - \hat{v}_{\lambda_i,i',j'}|) \right\}. \tag{10}$$

3.2 Determining the Optimal λ

According to Sec. 3.1, we first get the optical flow $(u_{\lambda_i}, v_{\lambda_i})$ by solving Eq. (10). Then we compare the RMS($u_{\lambda_i}, v_{\lambda_i}$) [Eq. (9)] of different λ_i to determine the optimal λ :

$$\lambda_{\text{optimal}} \rightarrow \min(RMS(u_{\lambda_i}, v_{\lambda_i})|_{i=1,2,\dots}). \tag{11}$$

Hence, the basic and most important step of the whole method is to set a group of λ_i .

In general, the relevance between λ_i and RMS($u_{\lambda_i}, v_{\lambda_i}$) isn't convex, which excludes using mathematical optimization algorithms for finding the optimal value. We propose a novel brute-force method similar to that described in Ref. 13, but much more efficient, especially when integrated with modern GPUs. In order to reduce the number of λ_i to be tested, we first choose a reference λ_0 , and then set a group of λ_i ($i = 1, 2, \dots$) around it in a specified range.

3.2.1 The principle used to select reference λ_0

According to our prior experiments on various sequences and the conclusions of other researchers,^{4,8} we define the following principle to use in choosing the reference λ_0 : first, the possible candidate values of λ_0 is [3; 5; 8; 12; 15; 20;

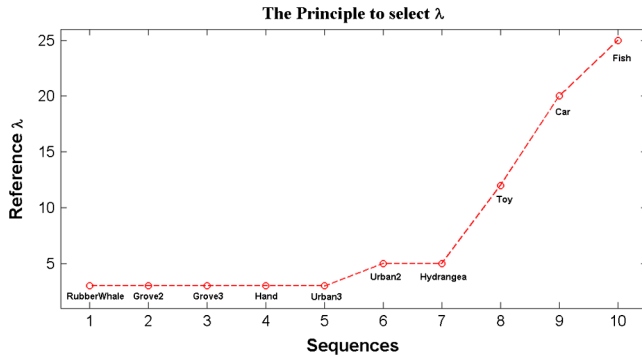


Fig. 1 The principle to select the reference value λ_0 .

25]; and second, λ_0 and its group sets are determined by the quality and resolution of the sequences. For high quality sequences, or the sequences with small details in the flow field, a small λ_0 is chosen. For low quality sequences with a rather smooth flow field, larger λ_0 should be selected. Figure 1 shows the principle to select the reference λ_0 .

3.2.2 The scheme to set the group λ_i

Zimmer⁶ has described a process wherein he incremented and decremented λ_0 by multiplying or dividing it with a stepping factor α several times. In contrast to this approach, we give a more suitable method to set the group of λ proportionally. For example, when selecting $\lambda_0 = 3$, the group of λ is set to $\lambda = [1:0.25:6]$, where the first and last value indicate the start and end point, respectively, and 0.25 indicates the step size between them. When selecting $\lambda_0 = 5$, the group of λ is set to $\lambda = [2:0.25:8]$. When selecting $\lambda_0 = 8$, the group of λ is set to $\lambda = [5:0.25:10:1/3:12]$ which indicates a step size of 0.25 between the starting point and 10, and a step size of 1/3 between 10 and the end point. When selecting $\lambda_0 = 12$, the group of λ is set to $\lambda = [8:0.25:10:1/3:16]$. When selecting $\lambda_0 = 15$, the group of λ is set to $\lambda = [10:1/3:20]$. When selecting $\lambda_0 = 20$, the group of λ is set to $\lambda = [15:1/3:20:0.5:25]$. When selecting $\lambda_0 = 25$, the group of λ is set to $\lambda = [20:0.5:30]$ and so forth. In contrast with Zimmer's approach, which prefers going from a smaller λ to a larger λ , this equal proportion set avoids testing smaller λ_i (left side of λ_0 , $\lambda_i < \lambda_0$) as well as less large λ_i (right side of λ_0 , $\lambda_i > \lambda_0$). As the range of λ is determined in a reasonable small scope, treating them equally avoids leaving out any requisite candidate.

3.3 Improved WRMS Approach

Although the RMS criterion is effective, it faces some problems: first, in practice, the sequences that require processing are often of low resolution and low quality (dim, noisy, etc.). Second, high quality sequences can contain serious occlusions, shadows, etc. In these cases, the accuracy of the flow field will deteriorate. Particularly, some wrong components ($u_{i,j}, v_{i,j}$) of the flow field can severely perturb the accuracy of the RMS method. Hence, we present a modified approach to improve its performance by introducing weighting to RMS. Intuitively, the reason for our choice is that if the flow field component ($u_{i,j}, v_{i,j}$) is wrong, the corresponding brightness in the error image $I_{(i,j)\text{Error}} = I_2[x + u_{i,j(\text{wrong})}, y + v_{i,j(\text{wrong})}] - I_1(x, y)$ will seriously deviate from the actual one $I_{(i,j)\text{right}} = I_2[x + u_{i,j(\text{right})}, y + v_{i,j(\text{right})}] - I_1(x, y)$.

Naturally, this results in its gradient $|\nabla I_{\text{Error}(i,j)\text{wrong}}|$ becoming much larger than the true gradient $|\nabla I_{(i,j)\text{right}}|$. We propose a weighted RMS (WRMS) criterion $|\nabla I_{\text{Error}(i,j)}|_{\text{WRMS}}$ to handle this problem, which gives a heavier weight to the wrong component, and a lower weight to the right one. This improvement makes our WRMS method to represent the error more precisely, especially under bad conditions.

Usually, people tend to directly use the gradient $|\nabla I|$ as a weight,¹⁸ and simply compute the forward difference, backward difference, or central difference. These differences are roughly calculated by subtracting the neighborhood pixels. When we use this ordinary method of calculating the gradient of the warped image $I_{\text{warp}} = I_2(x + u_{i,j}, y + v_{i,j})$, it results in some originally correctly warped pixels to show the wrong results. This occurs because, in the warped image, some correct pixels are surrounded with wrong pixels, especially in situations such as at the edges, noisy areas, discontinuity positions, occlusions, etc. For instance, $I_{\text{warp}(i,j)\text{wrong}} = I_{\text{warp}(i,j)\text{right}} - I_{\text{warp}(i-1,j)\text{wrong}}$. Reducing the number of these numerical approximation errors would further improve the result.

Through our research, we discovered that no correct pixel is isolated in the warped image $I_{\text{warp}} = I_2(x + u_{i,j}, y + v_{i,j})$. In other words, it is highly unlikely that a pixel is correct yet its neighbors are all wrong. At least some of its neighbors will be correct (for example, its upside neighbor is right, or both upside neighbor and forward neighbor are right, and so on). Basically, the brightness between the correctly warped pixel and its correctly warped neighbors is approximated, while a large difference exists between the correctly warped pixel and its relevant wrongly warped neighbors. Based on this characteristic, selecting the smaller of $[I_{x(i,j)} = \min(I_{x(i,j)\text{forward}}, I_{x(i,j)\text{backward}})]$ between the pixel's forward difference and backward difference can greatly reduce the wrong gradients $|\nabla I_{i,j}|$ (The same approach can be used to compute $I_{y(i,j)}$). Hence, the weight can be corrected by this way. This improvement can be verified in Table 1.

3.4 Principles to Reasonable Utilize WRMS, OPP

Using our WRMS method in complement with the state-of-the-art OPP method enables us to better deal with different practical conditions. With objects moving in a constant speed along a linear trajectory, the OPP approach should be considered first. Utilization of the WRMS method should be encouraged for sequences not possessing good quality as in the first case. Its use is strongly indicated especially where sequences have a significant amount of noise, serious occlusions, shadows, etc.

4 Experimental Results

We verified the correctness of our proposed WRMS approach by experiments using the Human-Assisted Motion Annotation database¹⁹ and the standard Middlebury benchmark database.³ In contrast with other papers^{4,6,8,11} which only test the artificial sequences, our experiments also include the real scene sequences.

In the first experiment, we check whether or not our improved gradient weight is effective. We compare both the average angular error (AAE) and average end-point error (EPE) of the following three methods with each other: our improved weighted RMS method (WRMS), the

Table 1 Contrast WRMS method to RMS method, central difference weight WRS (WRMS_C) method (Iteration = 1000).

	Hydrangea		RubberWhale		Grove2		Grove3		Urban2		Urban3		Hand		Toy		Car		Fish	
	AAE	EPE	AAE	EPE	AAE	EPE	AAE	EPE	AAE	EPE	AAE	EPE	AAE	EPE	AAE	EPE	AAE	EPE	AAE	EPE
RMS	1.8518	0.1535	2.4062	0.0767	1.4717	0.1042	4.8439	0.4565	1.9948	0.2136	3.3021	0.4069	14.5390	1.6709	2.4926	0.5665	5.2052	0.5043	15.8853	0.6338
WRMS_C	1.8518	0.1535	2.4062	0.0767	1.4157	0.0977	4.7976	0.4458	1.9948	0.2136	3.0768	0.4143	14.5336	1.6548	2.4988	0.5669	5.1510	0.5101	15.3927	0.6442
WRMS	1.8260	0.1531	2.4062	0.0767	1.4003	0.0977	4.7976	0.4458	1.9937	0.2120	3.0068	0.3943	14.5336	1.6548	2.4440	0.5622	5.1510	0.5101	15.3816	0.6313

general RMS method (without weight) (RMS), and the simple central difference weighted RMS method (WRMS_C). From Table 1, we can see that the weighted RMS method performs better than the pure RMS method, and our WRMS method further improves the accuracy of the simple WRMS_C method for most of the sequences.

In the second experiment, we check whether our WRMS method does automatically determine the optimal smoothness parameter λ . We compare the state-of-the-art “Classic+NL” algorithm, which uses the fixed smoothness parameter λ based on experience, with our WRMS method. Table 2 shows that our approach outperforms the “Classic+NL” algorithm in most of the examples. For some sequences, like Toy, Car, Fish, we find a surprised improvement. For these sequences, the suitable λ value was unknown, so the “Classic+NL” algorithm, which simply selects the λ without reference to experience and without setting it to a fixed value, is separated from practice. Instead, our WRMS method would automatically determine the optimal λ without ground truth and experience.

In the third experiment, we compare the performance of our WRMS method to automatically determine the optimal smoothness parameter λ with the state-of-the-art ADCE approach. The results presented in Table 3 show that our method is superior to the ADCE approach for most of the sequences, except for the high quality ones in which the primary motion of the objects are constant speed on a linear trajectory (like Hydrangea). For sequences (like Car, Fish) with a complex background and low resolution, our WRMS method still outperforms the ADCE approach, even if the objects move with a constant speed along a linear trajectory.

In these above three experiments, we selected the reference λ_0 according to our methodology outlined in Sec. 3.1. For the highest quality and resolution sequences, such as RubberWhale, Grove2, Grove3, Hand, Urban3, we set $\lambda_0 = 3$; For Urban2 and Hydrangea whose quality is a little lower than Urban3, we set a little higher value of $\lambda_0 = 5$. Based on this principle, we used the following values for other sequences: Toy, $\lambda_0 = 12$; Car, $\lambda_0 = 20$; Fish, $\lambda_0 = 25$.

In our last experiment, we investigate three complex real scene sequences from the Middlebury benchmark database which include occlusion, large displacement, small-scale structures, illumination changes, shadows, etc. (we use frame 9, frame 10, and frame 11 in the three sequences to be tested). We compare “Classic+NL” and ADCE methods with our approach to test the practicality and effectiveness of WRMS. In this test, we set $\lambda_0 = 12$ for the three sequences based on their quality.

Figure 2 shows that, when comparing the color optical flow field Figs. 2(a), 2(c), and 2(e) of the three methods, our WRMS method represents the complex movements of the legs almost completely correct, where the big girl’s legs are nearly totally occluded by the little girl. In Fig. 3, which compares the movement of the small balls in Figs. 3(a), 3(c), and 3(e), we can see that our approach performs much better than the other two methods. The warped frames Figs. 3(b), 3(d), and 3(f) reflect that the “Classic+NL” method and the ADCE method both fail to estimate the motion of the balls because it is hard to handle large displacements with small scale structures, as pointed out in

Table 2 Contrast WRMS method to Classic+NL⁸ method (Iteration = 1000).

	Hydrangea		RubberWhale		Grove2		Grove3		Urban2		Urban3		Hand		Toy		Car		Fish	
	AAE	EPE	AAE	EPE	AAE	EPE	AAE	EPE	AAE	EPE	AAE	EPE	AAE	EPE	AAE	EPE	AAE	EPE	AAE	EPE
Classic+NL	1.8338	0.1528	2.4062	0.0767	1.4042	0.1058	4.9173	0.4638	2.1382	0.2276	3.0589	0.3983	14.5669	1.6646	2.7917	0.5975	6.6106	0.5757	24.0588	0.8735
WRMS	1.8260	0.1531	2.4062	0.0767	1.4003	0.0977	4.7976	0.4458	1.9937	0.2136	3.0068	0.3943	14.5336	1.6548	2.4440	0.5622	5.1510	0.5101	15.3816	0.6313

Table 3 Contrast WRMS method to ADCE⁶ method (Iteration = 1000).

	Hydrangea		RubberWhale		Grove2		Grove3		Urban2		Urban3		Hand		Toy		Car		Fish	
	AAE	EPE	AAE	EPE	AAE	EPE	AAE	EPE	AAE	EPE	AAE	EPE	AAE	EPE	AAE	EPE	AAE	EPE	AAE	EPE
Classic+ADCE	1.8201	0.1525	2.4259	0.0773	1.4003	0.0977	5.1175	0.4917	2.0039	0.2118	3.3574	0.4118	14.6812	1.6901	2.4505	0.5647	5.2052	0.5043	15.8853	0.6338
WRMS	1.8260	0.1531	2.4062	0.0767	1.4003	0.0977	4.7976	0.4458	1.9937	0.2136	3.0068	0.3943	14.5336	1.6548	2.4440	0.5622	5.1510	0.5101	15.3816	0.6313

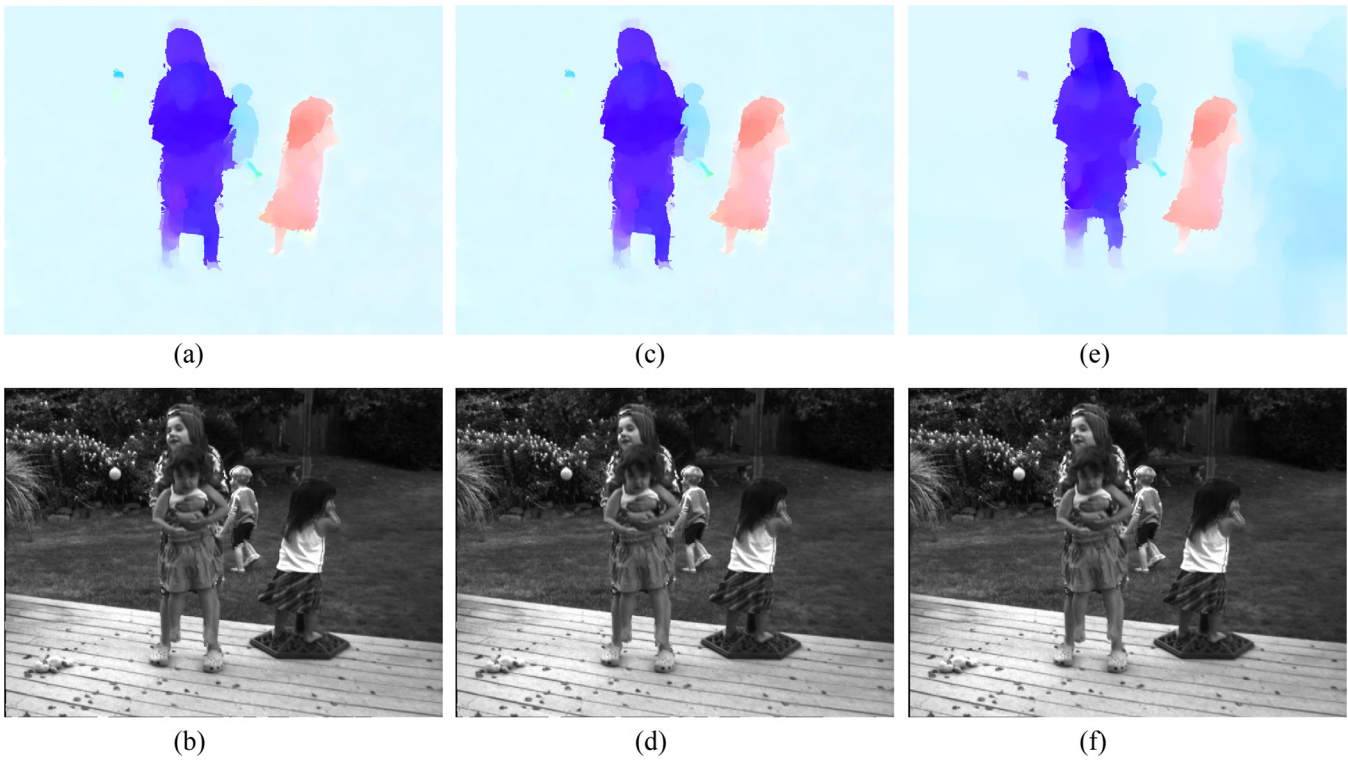


Fig. 2 The optical flow fields and the warped frames for the three methods applied to backyard sequences: (a) Backyard_Classic+NL_Colorflow, (b) Backyard_Classic+NL_Warp, (c) Backyard_ADCE_Colorflow, (d) Backyard_ADCE_Warp, (e) Backyard_WRMS_Colorflow, and (f) Backyard_WRMS_Warp.

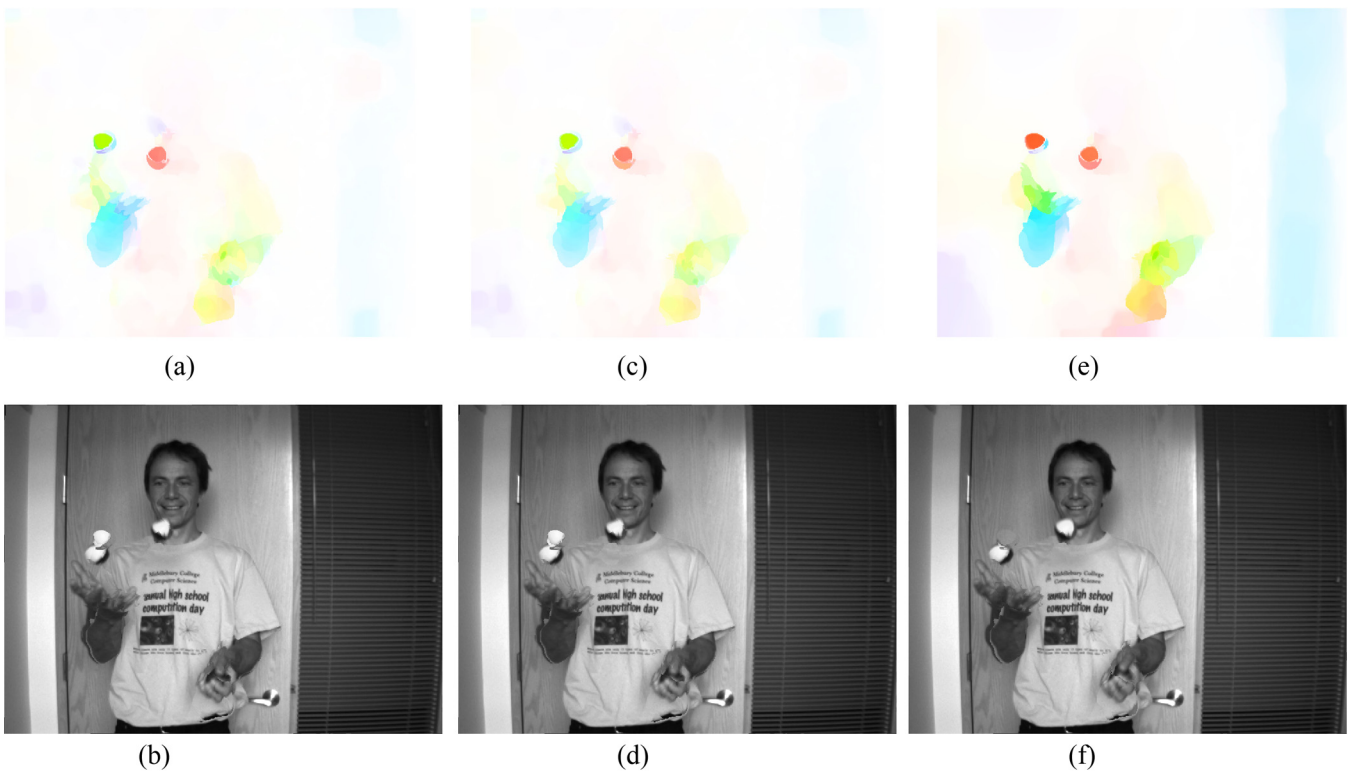


Fig. 3 The optical flow fields and the warped frames for the three methods applied to Beanbags sequences: (a) Beanbags_Classic+NL_Colorflow, (b) Beanbags_Classic+NL_Warp, (c) Beanbags_ADCE_Colorflow, (d) Beanbags_ADCE_Warp, (e) Beanbags_WRMS_Colorflow, and (f) Beanbags_WRMS_Warp.

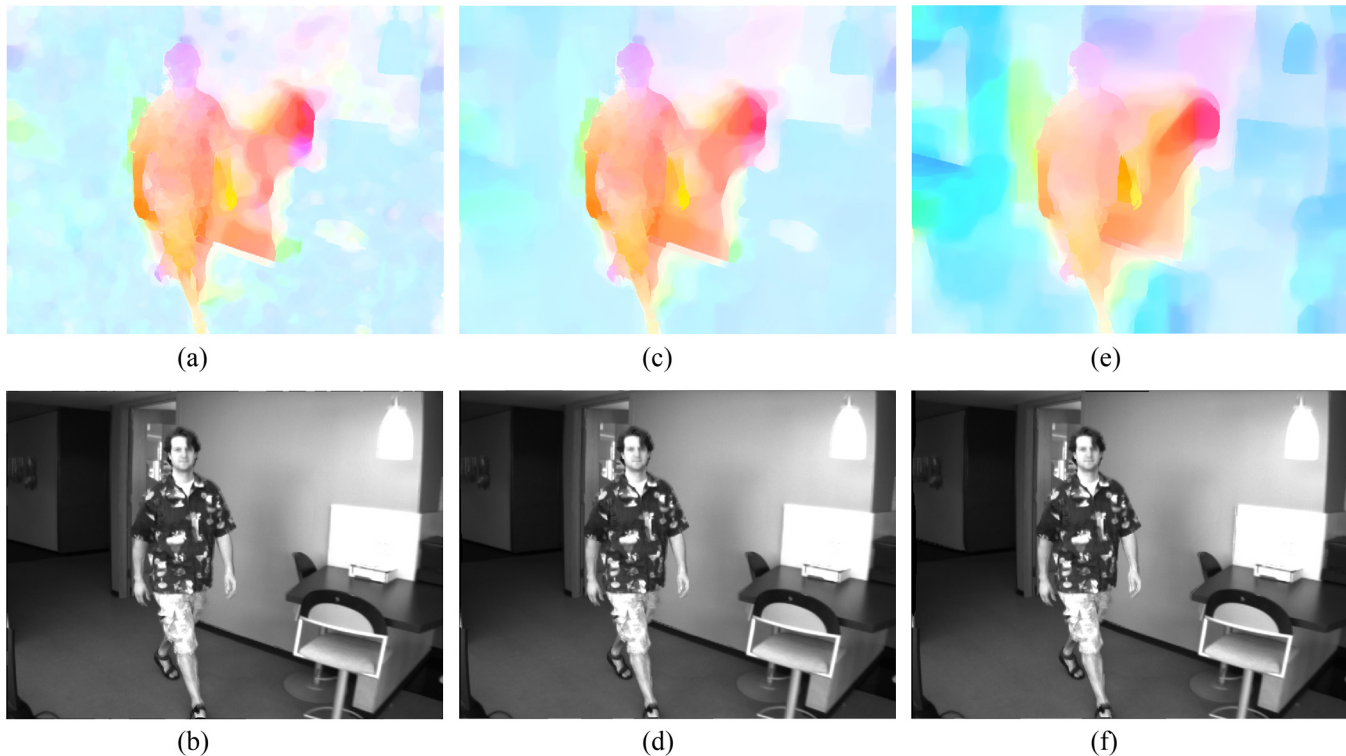


Fig. 4 The optical flow fields and the warped frames for the three methods applied to Walking sequences: (a) Walking_Classic+NL_Colorflow, (b) Walking_Classic+NL_Warp, (c) Walking_ADCE_Colorflow, (d) Walking_ADCE_Warp, (e) Walking_WRMS_Colorflow, and (f) Walking_WRMS_Warp.

Ref. 11. Our method solves this challenging problem. When comparing the primary motion of the man in Fig. 4, especially his left hand, and particularly the fingers and his shadow in Figs. 4(a), 4(c), and 4(e), we see that our flow field is much more accurate than the other two. Despite the complex sequences, which include illumination changes and shadows, our warped image (f) is nearly the same as the original frame.

The results of the five experiments indicate that our WRMS method can automatically determine the optimal smoothness parameter λ and improves the accuracy of the estimated flow field successful.

5 Conclusions

In this paper, we proposed an efficient WRMS method to automatically determine the optimal smoothness parameter λ , suitable for other kinds of variational optical flow algorithms. In our new approach, the reference λ_0 is set based on the quality of the frame and an effective way to assign a group of λ to be tested. The alternative gradient approach reduces numerical errors, further improves the weight of RMS, and also provides a new numerical way to calculate the derivative. Finally, we suggested how to employ the WRMS approach and the OPP method complementarily. Experimental results demonstrated the effectiveness of the presented approaches.

Acknowledgments

This research was supported by Natural Science Foundation of Hubei Province (2011CDB452), Natural Science

Foundation Key Program of Hubei Province (2009CDA141), National Key Technology R&D Program (2011BAK08B03) and special funds for basic research of Central Universities (111078).

References

1. B. Horn and B. Schunck, "Determining optical flow," *Artif. Intell.* **17**(1–3), 185–204 (1981).
2. C. Zach, T. Pock, and H. Bischof, "A duality based approach for real-time TV-L1 optical flow," *Proc. of the 29th DAGM Conf. on Pattern Recognition* **4713**(1), 214–223 (2007).
3. S. Baker et al., "A database and evaluation methodology for optical flow," *Int. J. Comput. Vis. (IJCV)* **92**(1), 1–31 (2011).
4. A. Bruhn et al., "Variational optical flow computation in real time," *IEEE Trans. Image Process* **14**(5), 608–615 (2005).
5. D. Sun et al., "Learning optical flow," in *European Conf. Computer Vision (IJCV)*, Springer-Verlag, Berlin, Heidelberg **3**, 83 (2008).
6. H. Zimmer, A. Bruhn, and J. Weickert, "Optic flow in harmony," *Int. J. Comput. Vis.* **93**(3), 368–388 (2011).
7. M. J. Black and P. Anandan, "The robust estimation of multiple motions: parametric and piecewise-smooth flow fields," *Comput. Vis. Image Understand.* **63**(1), 75–104 (1996).
8. D. Sun, S. Roth, and M. J. Black, "Secrets of optical flow estimation and their principles," *IEEE Conf. Comp. Vision Patt. Recognit.*, San Francisco, CA, pp. 2432–2439 (2010).
9. J. Molnár, D. Csetverikov, and S. Fazekas, "Illumination-robust variational optical flow using cross-correlation," *Comput. Vis. Image Understand.* **114**, 1104–1114 (2010).
10. B. D. Lucas and T. Kanade, "An iterative image registration technique with an application to stereo vision," in *Proc. of the Seventh International Joint Conf on Artificial Intelligence*, San Francisco, CA, USA, pp. 674–679 (1981).
11. T. Brox and J. Malik, "Large displacement optical flow: descriptor matching in variational motion estimation," *IEEE Trans. Pattern Anal.* **33**(3), 500–513 (2010).
12. N. P. Galatsanos and A. K. Katsaggelos, "Methods for choosing the regularization parameter and the noise variance in image restoration and their relation," *IEEE Trans. Image Process.* **1**(3), 322–336 (1992).

13. L. Ng and V. Solo, "A data-driven method for choosing smoothing parameters in optical flow problems," in *IEEE International Conf. on Image Processing*, Santa Barbara, CA, pp. 360–363 (1997).
14. K. Krajssek and R. Mester, "Bayesian model selection for optical flow estimation," *Pattern Recogn.* **47**(13), 142–151 (2007).
15. S. Baker and I. Matthews, "Lucas-Kanade 20 years on: a unifying framework," *Int. J. Comput. Vis.* **56**(3), 221–225 (2004).
16. L. I. Rudin, S. Osher, and E. Fatemi, "Nonlinear total variation based noise removal algorithms," *Phys. Nonlinear Phenom.* **60**(1–4), 259–268 (1992).
17. P. Sand and S. Teller, "Particle video: long-range motion estimation using point trajectories," *Int. J. Comput. Vis.* **80**(1), 72–91 (2008).
18. T. Ishikawa, I. Matthews, and S. Baker, "Efficient image alignment with outlier rejection," in: *Technique Report CMU-RI-TR-02-27*, Robotics Institute, Carnegie Mellon University (October 2002).
19. C. Liu et al. "Human-assisted motion annotation," *IEEE Conf. on Computer Vision and Pattern Recognition (CVPR)*, Anchorage, AK, pp. 1–8 (2008) <http://people.csail.mit.edu/ce-liu/motionAnnotation/>.



Zhigang Tu started his MPhil PhD in image processing in the School of Electronic Information, Wuhan University, China, 2008. Since September 2011, he has been with the Multimedia and Geometry Group at Utrecht University, Netherlands. His Current research interests include optical flow estimation, super-resolution construction, multimedia systems and technologies, human-computer interaction, and mobile computing.



Wei Xie received his BE degree in electronic information engineering and PhD degree in communication and information system from Wuhan University, China, in 2004 and 2010, respectively. He currently works at Computer School of Wuhan University, China. His research interests include super-resolution reconstruction, image fusion and image quality assessment.



Wolfgang Hürst is an assistant professor at the Department of Information and Computing Sciences at Utrecht University, Netherlands. His research interests include multimedia systems and technologies, human-computer interaction, mobile computing. Hürst has a PhD in computer science from the University of Freiburg, Germany, and a Masters in computer science from the University of Karlsruhe, Germany. From January 1996 to March 1997, he was a visiting researcher at Carnegie Mellon University in Pittsburgh, USA. From March 2005 through October 2007, he worked as research associate at the University of Freiburg, Germany.



Shufen Xiong is a graduate student in School of Electronic Information at Wuhan University, China. Her research interests are motion estimation and segmentation in computer vision.



Qianqing Qin received the PhD Degree in Science at NanKaiUniversity, China, in 1989. He held position of Assistant Professor in Huazhong University of Science and Technology from 1991 to 1995. Since 1995, he became a full professor at Ocean University of China. From 1999 through the present, he has been a professor in Wuhan University, China. His research interests include image processing, computer vision, and Wavelet computing.